

Wang Yi (Orcid ID: 0000-0001-5633-3312)
Hendy Ingrid (Orcid ID: 0000-0001-8305-6752)
Napier Tiffany, J (Orcid ID: 0000-0001-5982-8468)

Climate and anthropogenic controls of coastal deoxygenation on interannual to centennial timescales

Yi Wang¹, Ingrid Hendy*¹, and Tiffany J. Napier¹

¹ Department of Earth and Environmental Sciences, University of Michigan, Ann Arbor, MI 48109.

Corresponding author: Ingrid Hendy (ihendy@umich.edu)

Key Points:

- Annual reconstruction of Southern California oxygen minimum zone corroborated by unique linkage between sedimentary redox records and bottom water observations
- The 20th century anthropogenic warming trend plays a significant role in intensification of coastal deoxygenation on a centennial scale
- El Niño-Southern Oscillation contributes to interannual variability in extra-tropical oxygen minimum zones as a switch for ventilated and stagnant water columns

This is the author manuscript accepted for publication and has undergone full peer review but has not been through the copyediting, typesetting, pagination and proofreading process, which may lead to differences between this version and the [Version of Record](#). Please cite this article as doi: [10.1002/2017GL075443](https://doi.org/10.1002/2017GL075443)

Abstract

Understanding dissolved oxygen variability in the ocean is limited by the short duration of direct measurements, however sedimentary oxidation-reduction reactions can provide context for modern observations. Here we use bulk sediment redox-sensitive metal enrichment factors (M_{EF} , R_{EF} , and U_{EF}) and scanning X-ray fluorescence (XRF) records to examine annual-scale sedimentary oxygen concentrations in the Santa Barbara Basin from the Industrial Revolution (AD ~1850) to present. Enrichments are linked to measured bottom water oxygen concentrations after 1986. We reveal gradual intensification of the coastal oxygen minimum zone (OMZ) on the southern California margin coinciding the 20th century anthropogenic warming trend that leads to reduced oxygen solubility and greater stratification. High-frequency interannual oscillations become more prominent over the last three decades. These are attributed to local ‘flushing events’ triggered by the transition from El Niño to La Niña conditions, which further amplify changes in the extratropical southern Californian OMZ.

1 Introduction

As a critical component in marine environments, dissolved oxygen (DO) strongly modulates both metabolic and geochemical processes [Keeling *et al.*, 2010]. Reduced DO in the water column results in loss of biodiversity and sublethal stresses on surviving organisms (e.g., forced migration and reduction of habitats), especially in coastal marine ecosystems already impacted by pre-existing low- O_2 stresses [Bopp *et al.*, 2002; Deutsch *et al.*, 2014; Rabalais *et al.*, 2002; Vaquer-Sunyer and Duarte, 2008]. In a warming

ocean, declining O₂ in OMZs is attributed to lower gas solubility in the surface ocean and increased stratification, which reduces subsurface O₂ supply [Keeling and Garcia, 2002]. Primary productivity also plays a role as organic matter remineralization consumes significant O₂ in the ocean interior, and thus upwelling-induced high primary productivity regions often intersect with coastal OMZs. Human activities contribute to oxygen minimum zone (OMZ) expansion through anthropogenic climate change and eutrophication [Deutsch et al., 2014; Diaz and Rosenberg, 2008]. Nutrient-rich river discharge causes eutrophication, further stimulating phytoplankton growth, resulting in greater organic carbon flux and consequent O₂ loss. However, advection of oxygenated water into coastal OMZs replenishes stagnant, low-O₂ waters, counteracting eutrophication. Although ocean time series [McClatchie et al., 2010; Whitney et al., 2007] and repeated hydrological surveys [Bograd et al., 2008; Stramma et al., 2008] demonstrate statistically significant declines in water column DO, these measurements are limited by sparse sampling and short time series (<50 years).

Pre-instrumental OMZ changes are often reconstructed using sedimentary geochemical proxies, as DO controls redox-sensitive elemental concentrations in sediments during organic matter remineralization [Calvert and Pedersen, 2007; Scholz et al., 2014]. Following depletion of oxygen, sulfate eventually becomes the dominant electron acceptor in remineralization, resulting in accumulation of HS⁻ and facilitating redox-sensitive metal precipitation [Canfield and Thamdrup, 2009]. Here we use redox

metal enrichment factors (metal_{EF}) over local lithogenic background to track changes in the reducing environment of sediment porewaters (see Methods). Both Re and U have a negligible lithogenic background and are conservative in oxygenated waters, but are reduced to insoluble precipitates and enriched in sediments under low O_2 conditions [Crusius *et al.*, 1996; Tribovillard *et al.*, 2006]. In contrast, authigenic Mo precipitation proceeds only in the presence of free HS^- when O_2 concentrations are negligible, and thus indicates a strongly reducing environment [Crusius *et al.*, 1996]. As Re is preferentially scavenged under less reducing conditions, Re/Mo ratios are used to indicate changing redox conditions at the time of sediment deposition [Crusius *et al.*, 1996]. Sedimentary Re/Mo decreases when porewaters shift from slightly- to strongly-reducing sulfidic environments (free HS^- present).

As a near-shore basin in the southern California Bight, the Santa Barbara Basin (SBB) provides an ideal sedimentary archive for high-resolution reconstruction of the pre-instrumental OMZ from both climatic and anthropogenic perspectives. Measurements by the California Cooperative Oceanic and Fisheries Investigations (CalCOFI) indicate persistent low-oxygen concentrations (typically $<20 \mu\text{mol kg}^{-1}$) in the bottom water of central SBB. This low oxygen environment is inhospitable for most benthic mega- and macrofauna (notably burrowing organisms) except the sediment surface-dwelling gastropod *Alia permodesta* [Bernhard *et al.*, 2003; Bernhard *et al.*, 2000; Myhre *et al.*, 2017], preserving the seasonally distinct varved laminations for high-resolution

reconstructions [Schimmelmann *et al.*, 1990]. With a sill depth of ~450 m to the west, bottom water in the basin is either supplied from the California Undercurrent (CUC) [Bograd *et al.*, 2008; Lynn and Simpson, 1990; Nam *et al.*, 2015] or 'flushing events' - uplifted cold intermediate water [Auad *et al.*, 2003] that flush SBB when dense subsurface waters displace more buoyant water in the basin [Bograd, 2002]. Furthermore, due to its proximity to densely populated southern California, high-resolution sediment records in the SBB also make it possible to investigate abrupt OMZ responses to anthropogenic impacts.

Although extremely low oxygen concentrations in SBB are in part enhanced by silled bathymetry [Moffitt *et al.*, 2014], SBB still provides an model for near-shore basins in the Southern California Bight (e.g., Santa Monica Basin and San Pedro Basin) and physically connected to Baja California (eastern tropical northern Pacific, ETNP) via the CUC [Deutsch *et al.*, 2014; Kienast *et al.*, 2002]. Here we reconstruct the long-term and interannual OMZ responses to the global change since the Industrial Revolution in SBB sediments to understand processes controlling southern Californian OMZ variability, and to improve predictions of OMZ responses to human activities (Fig. 1). The core site has also been monitored quarterly by the CalCOFI since 1985. This provides direct measurements of bottom water properties for ~30 years and a unique linkage between the sedimentary record and water column observations.

2 Materials and Methods

The 67-cm box core SPR0901-04BC (34° 16.895' N, 120° 02.489' W, 588 m water depth) was recovered from SBB in January 2009 (Figs. 1 and S1). The basin is bounded by narrow sills to the west and east, with a depth of 475 m and 230 m, respectively (Figs. 1 and S1). SBB sediments are well-dated by radiometric methods and sediment fabric observations through ~40 years of frequent coring expeditions [Hendy *et al.*, 2015]. The sediment age model is based upon well-established varve counts [Schimmelmann *et al.*, 1990] and correlations to previously dated SBB cores using the same distinctive sedimentary fabric, notably varves associated with strong El Niño events in AD 1941, 1957, 1983, and 1997, two gray layers at 1761 and 1861-1862, the turbidite layer at 1812, and the *Macoma* bivalve layer at 1841 [Schimmelmann *et al.*, 1992]. Ages were then assigned to other samples based on the age model described above [Hendy *et al.*, 2015].

The core was scanned using an X-ray fluorescence (XRF) core scanner (Cox Analytical Instruments) at the Large Lakes Observatory, University of Minnesota, Duluth. The scanner was operated at 200- μ m resolution with an 8-second scan time using a Cr X-ray tube with a voltage of 30 kV and a current at 15 mA. The output results were recorded as counts per 8 seconds and are semi-quantitative [Croudace *et al.*, 2006; Hendy *et al.*, 2015]. Elemental XRF counts were normalized to Cr coherent scattering to isolate fluorescence intensity change from instrumental factors (for instance, tube aging) that may affect the primary beam intensity [Croudace *et al.*, 2006]. Ti, a conservative element

that is well-resolved by scanning XRF was employed as a normalizing element for terrigenous input [Croudace *et al.*, 2006], to isolate the authigenic redox signal from siliciclastic input. Sulfur counts were normalized to Cl, which is known to be conservative and representative of sea salts, to eliminate the influence of porewater salinity [Ziegler *et al.*, 2008].

For quantitative analyses, core SPR0901-04BC was sampled at continuous 1 cm intervals (~2-7 years) in spring 2013 to generate bulk samples [Hendy *et al.*, 2015]. The samples were freeze-dried and ground to <75 μm . 3-5 g of each powdered sample was sent to ALS Laboratories in Vancouver, Canada. The bulk samples were digested using nitric, perchloric, hydrofluoric, and hydrochloric cocktail. Quantitative analyses of major, minor and trace elements were conducted with inductively coupled plasma (ICP)-mass spectrometry and ICP-atomic emission spectroscopy (ICP-AES). Standard measurement errors for lab standards GBM908-10 and MRGeo08 are listed in Table S1.

Enrichment factors for redox-sensitive elements are calculated from measured sample concentrations and the regional lithogenic background value of SBB terrigenous sediment sources using the following equation [Turekian and Wedepohl, 1961]:

$$EF_i = \frac{(Element_i / Al)_{sample}}{(Element_i / Al)_{background}} \quad (1)$$

The mean background values of three sediment sources (Santa Clara River, Ventura River and the Channel Islands) were used to obtain a representative background lithogenic value for SBB sediments (for sample sites see Figs. 1 and S1; Table S3). The

weighted average value was calculated using a proportional sediment flux contribution of 0.78, 0.07 and 0.15 for the Santa Clara River, Ventura River and the Channel Islands, respectively [Warrick and Farnsworth, 2009].

To relate sedimentary redox proxies to bottom water observations, we used quarterly sampled bottom water nutrients and physical property data by CalCOFI from 1986 to 2015 at Station 81.8 46.9 (center of the basin, 34°16'29.64"N, 120°1'30"W at 557-578 m water depth), and station 80.0 55.0 (western sill depth, 34°19'N, 120°48'10.8"W at 500 m water depth) (Fig. 1 and Fig S1). Dissolved oxygen was determined using Winkler titrations [Carpenter, 1965], but this method was replaced by auto-titration measuring UV absorption of tri-iodide ion in 2003. Nutrients were measured with a colorimetric method on automated analyzers [Gordon *et al.*, 1993]. Detailed methods and data processing protocols can be found at www.calcofi.org.

ENSO phases are quantified by SST anomalies obtained from the Niño 3.4 Index (from NOAA, monthly SST from 5°N-5°S and 170°-120°W) after removing the mean value from 1951-2000. The CalCOFI bottom water temperature record sampled at 3-month intervals was interpolated to generate the same temporal resolution for correlation with monthly Niño 3.4 anomalies between 1986 and 2015 (n=349). Cross-correlation shows maximum correlation coefficient with 2-3 month lag at 95% confidence level (see Supplementary Information, Fig. S3). Here we use a response time of 3 months in relating ENSO perturbation to OMZ oscillations to account for the longer lag experienced

by subsurface upwelling sourced water as opposed to pycnocline depth anomalies [*Jacox et al.*, 2015].

3 Sedimentary oxygen reconstruction since the Industrial Revolution

Core SPR0901-04BC is a mostly laminated sequence except for the two identified gray layers (1761-1762 and 1861 flood) and one olive layer associated with the 1812 Santa Barbara earthquake [*Hendy et al.*, 2015]. It exhibits both long-term (centennial) evolution of reducing porewater conditions associated with regional warming trends [*Barron et al.*, 2013; *Field et al.*, 2006], and abrupt porewater responses to anthropogenic perturbations. Additionally, a high sedimentation rate (~2-3 mm/y) and seasonally distinct laminations allow for identification of interannual climate variability superimposed on the long-time (~150 year) OMZ evolution.

Before AD 1811, sedimentary laminations in the core demonstrate insufficient porewater O₂ for macrofauna. At ~1840 *Macoma* bivalve shells were found preserved *in situ* [*Schimmelmann et al.*, 1992]. These bivalves are intolerant of hypoxia (<65 μmol/kg) [*Coan*, 2000; *Myhre et al.*, 2017], indicating a relatively well-oxygenated benthic environment existed for <3 years. Less reducing sedimentary conditions at this time may have been attributed to the abrupt deposition of a seismically triggered turbidite in 1812 [*Borrero et al.*, 2001]. A pulse of metal oxides introduced into the deep basin, especially reactive Fe hydroxides, could have provided oxidants for free sulfides in bottom water. However, this interval also coincides with locally depressed sea surface temperatures

(SSTs) associated with the end of the Little Ice Age [Briffa *et al.*, 1998; Pak *et al.*, 2016]. Higher gas solubility and reduced water column stratification during early 19th century cooling may have led to redistribution of vertical zonation of ecosystems to allow benthic oxygenated ecosystems as O₂ increased on the margin [Moffitt *et al.*, 2015]. Our results cannot distinguish between these two possible scenarios, which additionally do not preclude each other. Suffocation of *Macoma* in ~1845 is supported by declining Re/Mo values and concomitant increasing Mo_{EF} (Fig. 2A and C), suggesting a return to low-oxygen conditions [Schimmelmann *et al.*, 1992].

The 1861-62 flood (~0.7 cm gray layer) [Hendy *et al.*, 2015] brought a pulse of oxygenated sediments into the basin that partly obscure the long-term trend towards more reducing porewater conditions (Fig. 2). However, from 1870 to ~1950 the average Mo_{EF} increased from 1.46 ± 0.12 (95% confidence level, prior to 1870) to 1.73 ± 0.08 with a concurrent Re/Mo decline from 2.55 ± 0.47 to 1.77 ± 0.09 , as Re_{EF} decreased from 3.73 ± 0.76 to 3.04 ± 0.18 and U_{EF} from 2.35 ± 0.24 to 2.13 ± 0.05 (Fig. 2A-D). This redox shift was decoupled from the sedimentary total organic carbon (TOC) concentrations, which remained mostly below average (~3.74 wt%) during this interval (Fig. 2E). Thus factors other than O₂ consumption by organic matter remineralization must have played a role in changing porewater redox chemistry. This long-term shift coincided with a rise in regional SSTs, as indicated by dinoflagellate cyst, foraminifera, coccolithophore, diatom and silicoflagellate census data [Barron *et al.*, 2013; Bringué *et al.*, 2014; De Bernardi *et*

al., 2008; *Field et al.*, 2006; *Grelaud et al.*, 2009]. Dinoflagellate taxa from SBB sediments suggest both warming SSTs and relaxation of upwelling conditions as early as the 1900s [*Bringué et al.*, 2014]. Diatoms also indicate 20th century warming, as assemblages shift toward larger diatom species around the 1940s [*Barron et al.*, 2013]. Anthropogenic 20th century warming could have led to a deeper thermocline and more intense stratification, reducing the O₂ supply to subsurface waters and providing a mechanism for the long-term shift toward more reducing conditions in the basin [*Di Lorenzo et al.*, 2005; *Keeling and Garcia*, 2002].

The sedimentary record also reveals the role of anthropogenic impacts on rapidly altering porewater redox chemistry, as indicated by sharp spikes in Mo_{EF} and a dramatic Re/Mo decline after 1950 and notably at 1969 (Fig. 2). These abrupt changes are clearly identified in the high-resolution Fe/Ti and S/Cl scanning XRF records. The sudden increase of sedimentary O₂ demand in 1969 may be associated with a well blowout in the Santa Barbara Channel that released ~420,000 gallons of crude oil following ~40 years of metal enriched drill oil discharge into SBB [*Foster et al.*, 1971]. A demand for porewater O₂ during the degradation of spilled hydrocarbon in this interval could have produced a dramatic shift toward more reducing porewater conditions. Similar sedimentary responses towards more reducing environments have also been observed in the Gulf of Mexico within the following two years after the *Deepwater Horizon* blowout

in 2010 [Hastings *et al.*, 2016], further addressing the role of anthropogenic perturbations on interannual oxygenation shifts in coastal areas.

After the 1970s, S/Cl and Fe/Ti records, in addition to redox sensitive metals, exhibit coincident oscillations (Fig. 2). Redox sensitive metal EFs, Mo in particular, become more coherent with sedimentary TOC content (correlation coefficient of 0.83, $n=12$, after 1969 compared to 0.66, $n=25$, between 1870-1969), suggesting organic matter remineralization controlled porewater redox changes that lead to rapid scavenging of redox elements near the sediment-water interface [Algeo and Lyons, 2006].

4 Water column observations and the sedimentary redox record

Comparison of independent, quarterly-sampled CalCOFI water chemistry time series to sub-annually sampled sedimentary scanning XRF records of redox-sensitive metals demonstrate annual-scale coherence from 1986 to 2010 (corresponding to ~7 cm depth in the sediment record). Nitrite spikes recorded (~4 and 7 $\mu\text{mol/kg}$ nitrite) in the summers of 2004 and 2005 were produced by denitrification in the local water column supported by concurrent decline of bottom water nitrate concentrations in the basin (Fig. 3C). Denitrification may have aggravated nitrogen loss in the water column and sharply altered the redox potential to facilitate redox metal precipitation. Coincident peaks in the subannually resolved scanning XRF Mo and Fe/Ti counts (Figs. 3A-B) confirm redox mineral preservation near the sediment-water interface that can be linked to highly active biogeochemical nutrient cycling in the water column. Thus, sedimentary redox proxies

are closely associated with water column oxygenation conditions, highlighting the validity of applying downcore records to reconstruct water column chemistry.

Furthermore, scanning XRF records have the potential to capture annually resolved redox changes.

5 Interannual dissolved oxygen concentrations and ENSO variability

Observed high frequency variability in redox metal concentrations suggests that other mechanisms beyond the centennial temperature-driven O₂ saturation may be important to DO concentrations. Both SBB sediment geochemistry and direct water column measurements display O₂ variability on an annual scale (Figs. 3 and 4) that can be attributed to interannual climate variability. Fig.4 demonstrates a tight linkage between ENSO variability and bottom water oxygen replenishment since 1986, notably through aforementioned 'flushing events' that control interannual bottom water O₂ concentrations and consequently impact the redox potential of sediment porewaters. When a 3-month lag is applied to the bottom water temperature and DO measurements relative to the Niño 3.4 temperature anomaly record, a significant correspondence (cross correlation $r=0.33$, 95% confidence level, see Supporting Information) is produced (Fig. 4). Rapid bottom water temperature decreases typically correspond to DO increases, suggesting external input of dense, cold and oxygenated water by flushing events. During El Niño years, bottom waters are typically anomalously warm (with a ~3 month response time). The concurrently depressed thermocline, weakened upwelling with shallower

source water depth [Jacox *et al.*, 2015], and the stronger CUC [Lynn and Bograd, 2002] contribute to a stagnant water column in SBB (lower frequency of flushing events, Fig. 4). With the transition from El Niño to La Niña conditions, invigorated upwelling flushes colder and more oxygenated intermediate water into the basin. Although flushing events are able to replenish water column O₂ instantaneously, SBB is only temporarily ventilated because subsequent remineralization of sinking organic matter quickly consumes the newly replenished O₂ in the bottom water (Fig. 4). Therefore, ENSO variability currently plays a role in rapidly switching the basin between the two oxygenation states (ventilated or stagnant) within several months. This highly oscillatory bottom water chemistry has contributed to the significant variability in porewater redox conditions over the past several decades. These results suggest short duration OMZ shifts can be predicted using ENSO indices providing several months of lead-time to assess potential ecological and environmental impacts on local ecosystems.

6 Conclusions

This high-resolution sediment archive extends dissolved oxygen (DO) instrumental measurements back in time and provides a unique insight into long-term evolution of the southern Californian coastal oxygen minimum zone (OMZ) since the Industrial Revolution (~1850). Enrichment of redox-sensitive metals in Santa Barbara Basin (SBB) sediments demonstrate aggravated reducing porewater environments that may result from the OMZ intensification through time. This centennial deoxygenation is

attributed to the warming of the North Pacific Ocean as primary productivity is shown to decouple from observed OMZ evolution. The 1969 oil spill in SBB is also recorded as a regional anthropogenic driven OMZ perturbation. Furthermore, interannual DO variability within the long-term deoxygenation trend is observed in both bottom water observations and the subannual scanning XRF elemental composition of sediments. 'Flushing event' frequency of SBB bottom waters is associated with interannual climate (ENSO) variability, which switches the basin between a stagnant and ventilated water column, further amplifying the OMZ variability.

Acknowledgments

This work is supported by the National Science Foundation under grant number OCE-1304327 awarded to I.H.; Y.W. and T.J.N. acknowledge support from the Rackham Graduate School of the University of Michigan. We would like to thank crews and scientists in CalCOFI for collecting high-quality data for decades and making it accessible to the public. CalCOFI data were freely obtained from <http://calcofi.org/data.html>. Other data are included as tables in the Supplementary Information.

References

- Algeo, T. J., and T. W. Lyons (2006), Mo-total organic carbon covariation in modern anoxic marine environments: Implications for analysis of paleoredox and paleohydrographic conditions, *Paleoceanography*, 21(1), 1-23.
- Awad, G., J. P. Kennett, and A. J. Miller (2003), North Pacific Intermediate Water response to a modern climate warming shift, *Journal of Geophysical Research*, 108(C11), 1-13.

Barron, J. A., D. Bukry, D. B. Field, and B. Finney (2013), Response of diatoms and silicoflagellates to climate change and warming in the California Current during the past 250 years and the recent rise of the toxic diatom *Pseudo-nitzschia australis*, *Quaternary International*, 310, 140-154.

Bernhard, J. M., P. T. Visscher, and S. S. Bowser (2003), Submillimeter life positions of bacteria, protists, and metazoans in laminated sediments of the Santa Barbara Basin, *Limnology and Oceanography*, 48(2), 813-828.

Bernhard, J. M., K. R. Buck, M. A. Farmer, and S. S. Bowser (2000), The Santa Barbara Basin is a symbiosis oasis, *Nature*, 403, 77-80.

Bograd, S. J. (2002), Bottom water renewal in the Santa Barbara Basin, *Journal of Geophysical Research*, 107(C12).

Bograd, S. J., C. G. Castro, E. Di Lorenzo, D. M. Palacios, H. Bailey, W. Gilly, and F. P. Chavez (2008), Oxygen declines and the shoaling of the hypoxic boundary in the California Current, *Geophysical Research Letters*, 35(12), 1-6.

Bopp, L., C. Le Quéré, M. Heimann, A. C. Manning, and P. Monfray (2002), Climate-induced oceanic oxygen fluxes: Implications for the contemporary carbon budget, *Global Biogeochemical Cycles*, 16(2), 1-13.

Borrero, J. C., J. F. Dolan, and C. E. Synolakis (2001), Tsunamis within the Eastern Santa Barbara Channel, *Geophysical Research Letters*, 28(4), 643-646.

Briffa, K. R., P. D. Jones, F. H. Schweingruber, and T. J. Osborn (1998), Influence of volcanic eruptions on Northern Hemisphere summer temperature over the past 600 years, *Nature*, 393, 450-455.

Bringué, M., V. Pospelova, and D. B. Field (2014), High resolution sedimentary record of dinoflagellate cysts reflects decadal variability and 20th century warming in the Santa Barbara Basin, *Quaternary Science Reviews*, 105, 86-101.

Calvert, S. E., and T. F. Pedersen (2007), Elemental Proxies for Palaeoclimatic and Palaeoceanographic Variability in Marine Sediments: Interpretation and Application, in *Developments in Marine Geology*, edited, pp. 567-644.

Canfield, D. E., and B. Thamdrup (2009), Towards a consistent classification scheme for geochemical environments, or, why we wish the term 'suboxic' would go away, *Geobiology*, 7(4), 385-392.

Carpenter, J. H. (1965), The Chesapeake Bay Institute Technique for the Winkler dissolved oxygen method, *Limnology and Oceanography*, 10(1), 141-143.

Coan, E. V. (2000), The eastern Pacific Recent species of the bivalve genus *Gari* (Tellinoidea: Psammobiidae), with notes on western Atlantic and fossil taxa, *Malacologia*, 42(1-2), 1-29.

Croudace, I. W., A. Rindby, and R. G. Rothwell (2006), ITRAX: description and evaluation of a new multi-function X-ray core scanner, *Geological Society, London, Special Publications*, 267(1), 51-63.

Crusius, J., S. Calvert, T. Pedersen, and D. Sage (1996), Rhenium and molybdenum enrichments in sediments as indicators of oxic, suboxic and sulfidic conditions of deposition, *Earth and Planetary Science Letters*, 145, 65-78.

De Bernardi, B., P. Ziveri, E. Erba, and R. C. Thunell (2008), Calcareous phytoplankton response to the half century of interannual climatic variability in Santa Barbara Basin (California), *Paleoceanography*, 23(2), 1-13.

Deutsch, C., et al. (2014), Centennial changes in North Pacific anoxia linked to tropical trade winds, *Science*, 345(6197), 665-668.

Di Lorenzo, E., A. J. Miller, N. Schneider, and J. C. McWilliams (2005), The Warming of the California Current System- Dynamics and Ecosystem Implications, *Journal of Physical Oceanography*, 35, 336-362.

Diaz, R. J., and R. Rosenberg (2008), Spreading dead zones and consequences for marine ecosystems, *Science*, 321(5891), 926-929.

Field, D., T. R. Baumgartner, C. D. Charles, V. Ferrelra-Bartrina, and M. D. Ohman (2006), Planktonic foraminifera of the California Current reflect 20th-century warming, *Science*, 311, 63-66.

Foster, M., A. C. Charters, and M. Neushul (1971), The Santa Barbara oil spill Part 1: initial quantities and distribution of pollutant crude oil, *Environmental Pollution*, 2, 97-113.

Gordon, L. I., J. C. J. Jennings, A. A. Ross, and J. M. Krest (1993), A Suggested Protocol for Continuous Flow Automated Analysis of Seawater Nutrients in the WOCE Hydrographic Program and the Joint Global Ocean Fluxes Study *Rep.*, WOCE Hydrographic Program Office.

Grelaud, M., A. Schimmelmann, and L. Beaufort (2009), Coccolithophore response to climate and surface hydrography in the Santa Barbara Basin, California, AD 1917-2004, *Biogeosciences*, 6, 2025-2039.

Hastings, D. W., P. T. Schwing, G. R. Brooks, R. A. Larson, J. L. Morford, T. Roeder, K. A. Quinn, T. Bartlett, I. C. Romero, and D. J. Hollander (2016), Changes in sediment redox conditions following the BP DWH blowout event, *Deep Sea Research Part II: Topical Studies in Oceanography*, 129, 167-178.

Hendy, I. L., T. J. Napier, and A. Schimmelmann (2015), From extreme rainfall to drought: 250 years of annually resolved sediment deposition in Santa Barbara Basin, California, *Quaternary International*.

Jacox, M. G., J. Fiechter, A. M. Moore, and C. A. Edwards (2015), ENSO and the California Current coastal upwelling response, *Journal of Geophysical Research: Oceans*, 120, 1691-1702.

Keeling, R. E., and H. E. Garcia (2002), The change in oceanic O₂ inventory associated with recent global warming, *Proceedings of the National Academy of Sciences of the United States of America*, 99(12), 7848-7853.

Keeling, R. E., A. Kortzinger, and N. Gruber (2010), Ocean deoxygenation in a warming world, *Annual review of marine science*, 2, 199-229.

Kienast, S. S., S. E. Calvert, and T. F. Pedersen (2002), Nitrogen isotope and productivity variations along the northeast Pacific margin over the last 120 kyr: Surface and subsurface paleoceanography, *Paleoceanography*, 17(4), 7-1-7-17.

Lynn, R. J., and J. J. Simpson (1990), The flow of the undercurrent over the continental borderland off southern California, *Journal of Geophysical Research*, 95(C8), 12995-13008.

Lynn, R. J., and S. J. Bograd (2002), Dynamic evolution of the 1997–1999 El Niño–La Niña cycle in the southern California Current System, *Progress in Oceanography*, 54, 59-75.

McClatchie, S., R. Goericke, R. Cosgrove, G. Auad, and R. Vetter (2010), Oxygen in the Southern California Bight–Multidecadal trends and implications for demersal fisheries, *Geophysical Research Letters*, 37(L19602), 1-5.

Moffitt, S. E., T. M. Hill, P. D. Roopnarine, and J. P. Kennett (2015), Response of seafloor ecosystems to abrupt global climate change, *Proc Natl Acad Sci U S A*, 112(15), 4684-4689.

Moffitt, S. E., T. M. Hill, K. Ohkushi, J. P. Kennett, and R. J. Behl (2014), Vertical oxygen minimum zone oscillations since 20 ka in Santa Barbara Basin: A be

Paleoceanography, 29(1), 44-57.

Myhre, S. E., K. J. Kroeker, T. M. Hill, P. Roopnarine, and J. P. Kennett (2017), Community benthic paleoecology from high-resolution climate records: Mollusca and foraminifera in post-glacial environments of the California margin, *Quaternary Science Reviews*, 155, 179-197.

Nam, S., Y. Takeshita, C. A. Frieder, T. Martz, and J. Ballard (2015), Seasonal advection of Pacific Equatorial Water alters oxygen and pH in the Southern California Bight, *Journal of Geophysical Research: Oceans*, 120(5387-5399).

Pak, D. K., I. L. Hendy, J. C. Weaver, A. Schimmelmann, and L. Clayman (2016), Foraminiferal proxy response to ocean temperature variability and acidification over the last 150 years in the Santa Barbara Basin (California), *Quaternary International*.

Rabalais, N. N., R. E. Turner, and W. J. Wiseman (2002), Gulf of Mexico Hypoxia, A.K.A. “The Dead Zone”, *Annual Review of Ecology and Systematics*, 33(1), 235-263.

Ryan, W. B. F., et al. (2009), Global Multi-Resolution Topography synthesis, *Geochemistry, Geophysics, Geosystems*, 10(3), 1-9.

Schimmelmann, A., C. B. Lange, and W. H. Berger (1990), Climatically controlled marker layers in Santa Barbara Basin sediments and fine-scale core-to-core correlation, *Limnology and Oceanography*, 35(1), 165-173.

Schimmelmann, A., C. Lange, W. H. Berger, A. Simon, S. K. Burke, and R. B. Dunber (1992), Extreme climatic conditions recorded in Santa Barbara Basin laminated sediments: the 1835–1840 Macoma event, *Marine Geology*, 106(1992), 279-299.

Schlitzer, R. (2000), Electronic atlas of WOCE hydrographic and tracer data now available, *Eos, Transactions American Geophysical Union*, 81(5), 45-45.

Scholz, F., J. McManus, A. C. Mix, C. Hensen, and R. R. Schneider (2014), The impact of ocean deoxygenation on iron release from continental margin sediments, *Nature Geoscience*, 7(6), 433-437.

Stramma, L., G. C. Johnson, G. C. Sprintall, and V. Mohrholz (2008), Expanding Oxygen-Minimum Zones in the Tropical Oceans, *Science*, 320(5876), 655-658.

Tribouillard, N., T. J. Algeo, T. Lyons, and A. Riboulleau (2006), Trace metals as paleoredox and paleoproductivity proxies: An update, *Chemical Geology*, 232(1-2), 12-32.

Turekian, K., and K. H. Wedepohl (1961), Distribution of the Elements in Some Major Units of the Earth's Crust, *Geological Society of America Bulletin*, 72, 175-192.

Vaquier-Sunyer, R., and C. M. Duarte (2008), Thresholds of hypoxia for marine biodiversity, *Proceedings of the National Academy of Sciences of the United States of America*, 105(40), 15452-15457.

Warrick, J. A., and K. L. Farnsworth (2009), Sources of sediment to the coastal waters of the Southern California Bight, *The Geological Society of America Special Paper*, 454, 39-52.

Whitney, F. A., H. J. Freeland, and M. Robert (2007), Persistently declining oxygen levels in the interior waters of the eastern subarctic Pacific, *Progress in Oceanography*, 75(2), 179-199.

Ziegler, M., T. Jilbert, G. J. de Lange, L. J. Lourens, and G.-J. Reichert (2008), Bromine counts from XRF scanning as an estimate of the marine organic carbon content of sediment cores, *Geochemistry, Geophysics, Geosystems*, 9(5), 1-6.

Author Manuscript

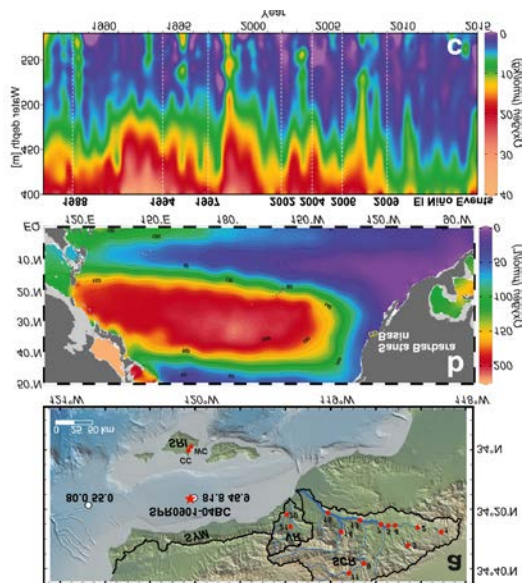


Figure 1. Study area and oxygen time series. (a) Map of the Santa Barbara Basin (SBB). The red star denotes the core site of SPR0901-04BC while the two white circles represent the CalCOFI stations (81.8 46.9 [34.27490°N, 120.02524°W] and 80.0 55.0 [34.31667°N, 120.80245°W]). River catchments are outlined in black. Main stems of selected rivers are indicated by thick blue lines: Santa Clara River (SCR), Ventura River (VR), Santa Ynez Mountain (SYM), and Santa Rosa Island (SRI). Lithogenic background sample sites are shown in red circles. Bathymetry is from Global Multi-Resolution Topography version 2.6 [Ryan *et al.*, 2009]. (b) Color shaded contour map shows the oxygen concentration ($\mu\text{mol/L}$) at 400 m water depth. SBB is denoted with a yellow box. Data are from the World Ocean Atlas 2013 on a 1° longitude \times 1° latitude grid; (c) Intermediate-depth O₂ concentration time series ($\mu\text{mol/kg}$) from 1985 to 2015 at the

center of SBB, indicating highly variable oxygen concentrations. Selected El Niño events are highlighted with white dashed lines. Data are obtained from CalCOFI station 81.8

46.9. Maps and profiles are generated from Ocean Data View [Schlitzer, 2000].

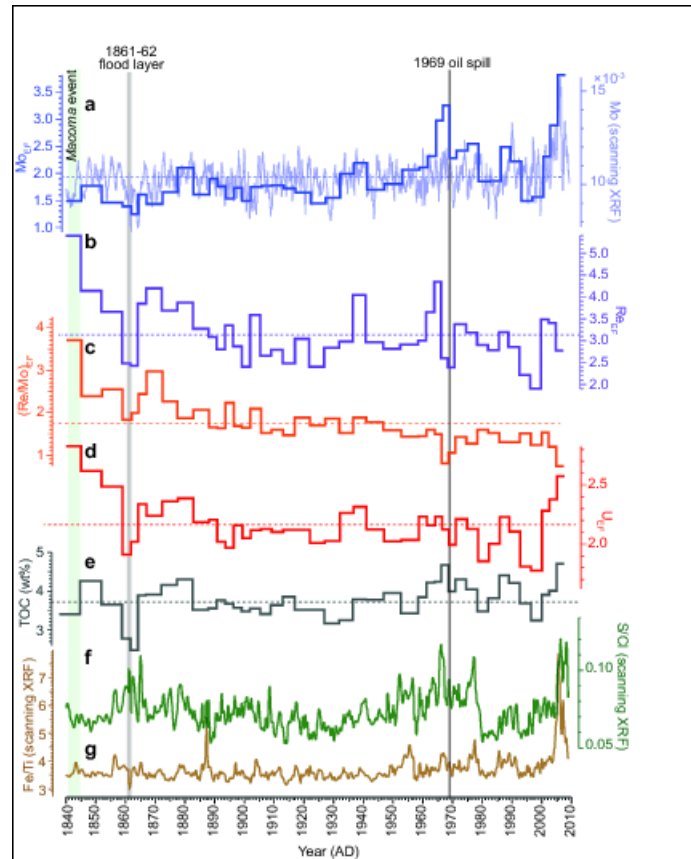


Figure 2. Enrichment factors (EFs) of redox proxies and average values for the last 170 years: (a) Mo_{EF} (thick blue line), the average value of Mo_{EF} (blue dashed line), and 20-pt moving average of scanning XRF Mo normalized to Cr coherent scattering (thin blue line); (b) Re_{EF} (thick purple line) and average value (purple dashed line); (c) Re_{EF}/Mo_{EF}

ratio (thick orange line) and average value (orange dashed line); (d) U_{EF} (thick red line) and average value (red dashed line); (e) TOC (wt. %, thick gray line) and mean value (gray dashed line) [Hendy *et al.*, 2015]; (f-g) The 20-pt moving average of scanning XRF Fe/Ti (brown line) and S/Cl (green line); The *Macoma* bivalve layer (green shading), 1861-62 flood layer (gray bar), and 1969 oil spill event (black line) are indicated.

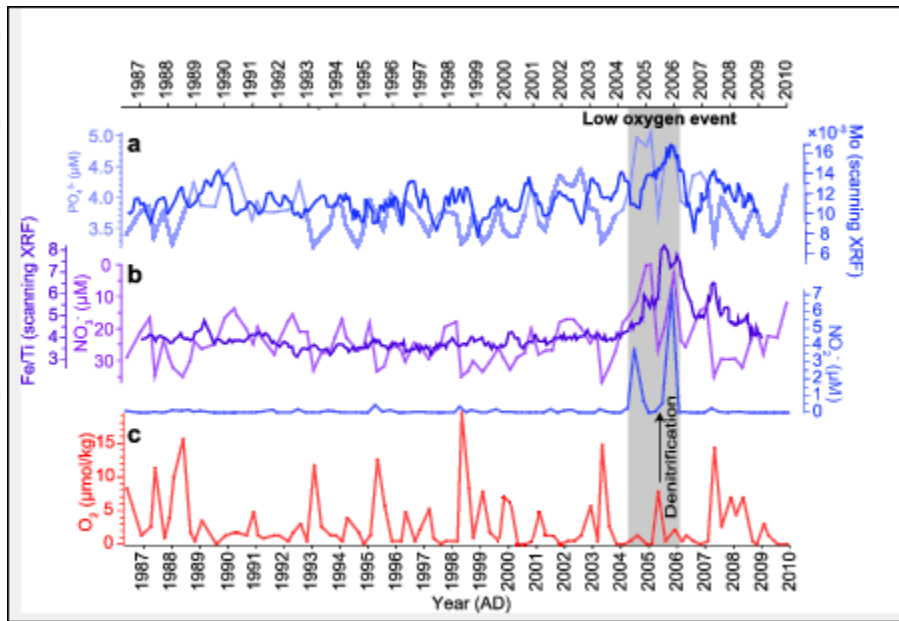


Figure 3. Bottom water properties of Santa Barbara Basin (SBB) and redox proxies. (a) Bottom water phosphate ($\mu\text{mol/L}$, thick light blue line) and the 5-pt moving average of normalized scanning XRF Mo (thin blue line) normalized to Cr coherent scattering; (b) Nitrate ($\mu\text{mol/L}$, light purple line), 5-point moving average of Fe/Ti (dark purple line), and nitrite ($\mu\text{mol/L}$, light blue line); (c) Dissolved oxygen of bottom water ($\mu\text{mol/kg}$, red line). Water chemistry and temperature data are obtained from California Cooperative

Oceanic Fisheries Investigations (CalCOFI). The low oxygen event is indicated by gray shading.

Author Manuscript

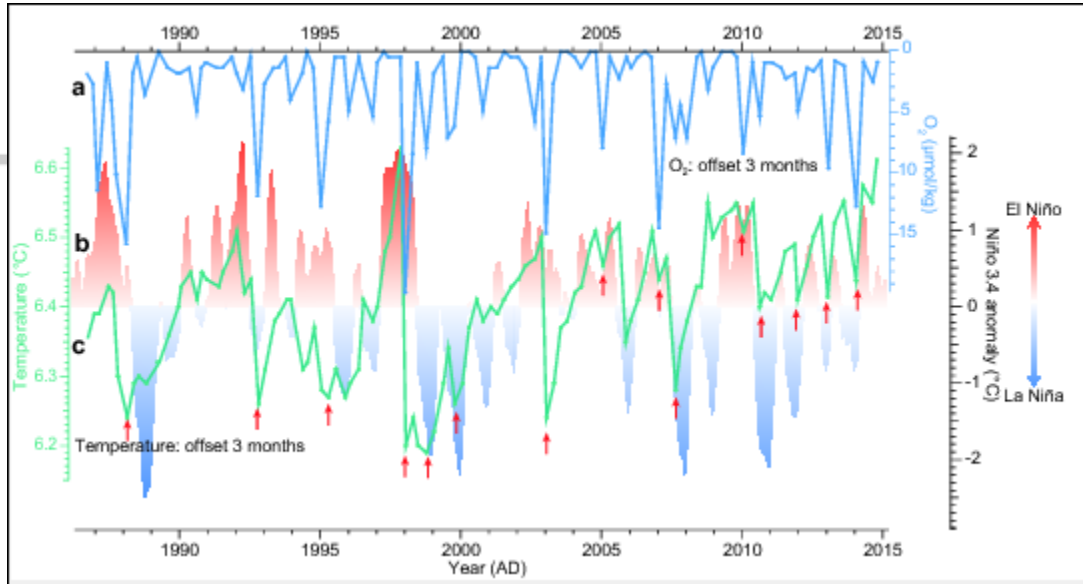


Figure 4. Relationship between bottom water temperature, oxygen concentration and ENSO variability. (a) Dissolved oxygen of bottom water (blue line, $\mu\text{mol/kg}$) at station 81.8 46.9 (water depths between 557-578 m used; data offset of 3 months applied); (b) Bottom water temperature at the same station denoted as the green line ($^{\circ}\text{C}$, data offset of 3 months applied); (c) Red (El Niño) and blue (La Niña) shading represent Niño 3.4 anomalies as indicators of ENSO variability. Red arrows indicate flushing events that correspondent to abrupt water temperature decreases.